Materials Letters 412 (2026) 140428

Contents lists available at ScienceDirect

Materials Letters

journal homepage: www.elsevier.com/locate/matlet

Recommended solutions for the disinfection of Ti-Zr-Cu-Pd bulk metallic glasses

C. Torres-Sanchez *, S. Yang, J. Tarum, P.P. Conway

Multifunctional Materials Manufacturing Lab, Wolfson School, Loughborough University, LE11 3TU, Loughborough, Leics, UK

ARTICLE INFO

Keywords:
Bulk metallic glass
Ti-Zr-Cu-Pd
Disinfection
NaClO
NaOH
Osteoblast

ABSTRACT

Disinfection of medical devices is crucial to patient safety. Notably, an incorrect selection of disinfectant can damage the material surface and impact its performance. Ti-Zr-Cu-Pd bulk metallic glasses (BMGs) show considerable potential for biomedical use, however standard sterilisation protocols remain undeveloped. This study evaluates the effects of common clinical disinfection solutions, including NaOH, NaClO, and Virkon®, on Ti-Zr-Cu-Pd BMGs, to assess their impact on surface characteristics (chemical composition, surface free energy) and on biocompatibility (pre-osteoblast cells behaviour). The findings aim to inform practical guidelines for safe and effective cleaning and sterilisation of devices that contain these alloys.

1. Introduction

Bulk Metallic Glasses (BMGs) are undercooled 'frozen liquids'; very rapid cooling to a temperature below glass transition makes them amorphous when solidified. The absence of crystal structure and grain boundaries imply that metallic bonding-related dislocations and atom-array failure modes are not exhibited. Therefore, their mechanical properties are superior to those of their crystalline counterparts. Ti-Zr-Cu-Pd BMGs have attracted attention as materials for implantable devices because their composition does not include Al, V, Cr, Co elements [1], their mechanical strength and yield strain are high, Young's modulus is low, and their oxide layer enhances cell behaviour [2,3]. Sterilisation of medical implants is vital to prevent bacterial growth and infection in the host tissue. As new materials enter the selection palette for medical devices and instruments manufacture [2], the material-disinfectant pair selection is critical. Sodium hydroxide (NaOH) is used to decontaminate surgical instruments [4], sodium hypochlorite (NaClO) is typically used as endodontic irrigant [5], and non-chlorinated oxidants such as potassium peroxymerosulphate triple salt (e.g., Virkon®) are broadly used on surfaces where pathogen control is necessary. Domestic bleach (i.e., NaOH/NaClO mixture) is also used in surgical settings as disinfectant.

In this study a Ti-Zr-Cu-Pd BMG was exposed to commonly used antibacterial and biocide solutions to assess their impact on surface chemistry, and how this influenced the behaviour of pre-osteoblasts attachment and proliferation stage. Immediate practical application includes disinfection recommendations in dental orthodontics and surgery.

2. Materials and methods

Rods (3 mm diameter, composition $Ti_{42}Zr_8Cu_{42}Pd_8$ (at.%)) were prepared from elements (purity ≥99.9%, ThermoFisherScientific, UK) by arc melting and suction casting (MAM-1, Edmund-Bühler, Germany). Full amorphicity was confirmed [3]. Sliced discs (1.5 mm thickness) were polished (P400/P600/P1200 paper (AutoMet 250, Buehler, Germany)) to obtain a baseline surface roughness of R_a (6.78 ± 0.75 μm) and R_z (27.89 ± 4.57μm). They were immersed (24 h, room temperature) in 1 M NaOH, 0.134 M (equiv. 1%) NaClO, a mixed solution comprising 1 M NaOH and 1% NaClO, or 1% Virkon (Fisher Sci., UK). Higher concentrations of those solvents resulted in excessive damage of the surfaces (Supplementary material). The 24 h exposure simulated intense cleaning routines in the abatement of persistent spores and inactivation of microorganisms. Untreated discs served as control. Characterisation included X-ray photoelectron (XPS, K-alpha, ThermoScientific, UK), energy-dispersive X-ray spectroscopy (EDX), scanning microscopy (SEM) (JEOL JSM-7800F, Japan), wettability (sessile drop) and Surface Free Energy (SFE) (via OWRK method) [6].

MC3T3-E1 (passage 15, ECACC, 300 cells/mm^2) seeded on the discs were incubated for 9 days in complete medium (Minimum Essential Medium (MEM), 10% fetal bovine serum (FBS), 1% penicillin-streptomycin and 1% GlutaMAX™ (Gibco, UK)). PrestoBlue™ Cell

* Corresponding author.
E-mail address: c.torres@lboro.ac.uk (C. Torres-Sanchez).

https://doi.org/10.1016/j.matlet.2026.140428
Received 21 January 2026; Received in revised form 2 March 2026; Accepted 7 March 2026
Available online 9 March 2026

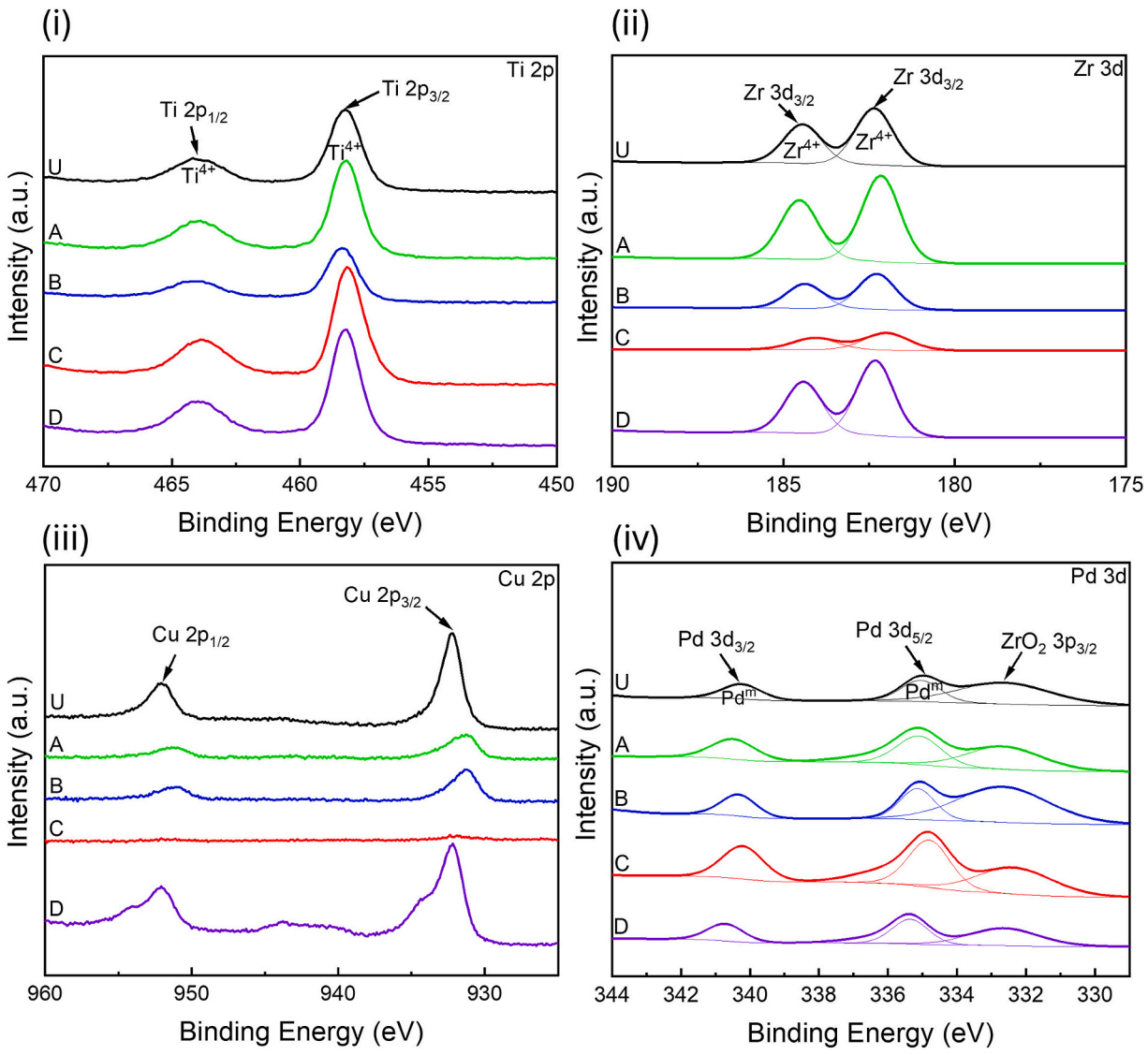

Fig. 1. Deconvoluted core-level XPS spectra of (i) Ti2p, (ii) Zr3d, (iii) Cu2p and (iv) Pd3d for the untreated (U) and treated (A-D) surfaces with the four disinfectants.

Viability Reagent (Invitrogen™, UK) was used as a surrogate for cell number (via the standard curve from fluorescence values (Ex 560/Em 590)) [6]. Readings were performed every 48 h. Staining with 0.01% Toluidine Blue solution (Sigma, UK) allowed morphology observation on day 5 (Nikon SMZ25, NL).

Measurements in triplicate reported means ± SD. One-way ANOVA using Shapiro normality tests were used for the statistical analysis. A value $p \leq 0.05$ was considered significant.

3. Results and discussion

The surfaces were characterised to understand the chemical and physical changes after exposure to the different disinfectants. The XPS deconvolution spectra of Ti2p, Zr3d, Cu2p (Fig. 1i-iii) indicate the presence of their oxide species, and for Pd 3d (Fig. 1iv) in its metal species. After treatment with NaOH the intensity of Cu2p peaks decreased, Zr3d peaks increased, with less noticeable changes to Ti2p and Pd3d peaks. When the samples were treated with NaClO the peak intensity of Ti2p, Zr 3d and Cu2p decreased and the Pd3d increased. These results agree with the oxide layers composition (Table 1). While the Cu_xO was removed from the surface exposing the Pd(0) metal, the attack mechanism was different for the two disinfectants. The species formed from the dissolution of NaOH interacted with the surface through hydrolysis (Eq. 1) and the increase of Pd(0) was accompanied by an increase also in ZrO_2 and TiO_2, a robust self-passivation layer. Conversely, when Cl^- ions were present, the dismantling of the Cu oxide layer (via an anodic mechanism, Eq. 2 [7]) was less marked, and the depletion in Cu_xO was accompanied by Pd(0) increase and TiO_2 decrease.

$$Cu^{2+}{}_{aq} + 2\,OH^-{}_{aq} \rightarrow Cu(OH)_{2\ solid}\ (\text{blue, precipitate}) \quad (1)$$

$$Cu^{+}{}_{aq} + Cl^-{}_{aq} \rightarrow CuCl\ (\text{insoluble, brief lifespan}) + Cl^- \rightarrow CuCl^-{}_2\ (\text{soluble complex}) \quad (2)$$

When NaOH and NaClO were mixed their effect was synergistic; the Cu and Zr oxides were depleted leaving the outermost layer enriched in TiO_2 and Pd(0) (Fig. 1, Table 1). Cuprous oxide was attacked by both OH^- and Cl^- ions, forming soluble complexes ($Cu(OH)_2$ ($\Delta H°_f$ = −611.5 kJ/mol) and $CuCl_2$ (−220.1 kJ/mol)) and doubling the consumption of Cu^{x+} ions, expediting metal dissolution. Furthermore, cuprous oxide production in the presence of Cl^- ions is a precipitation reaction (Eq. 3) of right-shifted equilibrium when the concentration of $[CuCl_2^-]$ species increases [8]; Cu_2O was deposited in response, hence increasing Cu concentration in pitting cavities (Fig. 2ix, xiii). The formation of $Zr(OH)_4$ (arising from the dissociation of NaOH, Eq. 4) is very

Table 1
Chemical composition, physical and biocompatibility properties of the surfaces.

	Untreated	1 M NaOH	1% NaClO	1 M NaOH + 1% NaClO	1% Virkon
Label	U	A	B	C	D
Oxide layer composition (at. %)					
TiO_2	66.08	69.05	60.08	76.86	64.30
ZrO_2	9.48	15.65	9.58	3.38	12.36
Cu_xO	21.83	9.14	15.74	2.06	19.69
Pd (metal)	2.61	6.16	14.60	17.70	3.65
Contact angle (°)					
DI water	67.3 ± 2.5	44.2 ± 3.6	82.3 ± 3.7	48.9 ± 2.9	61.0 ± 1.9
Surface free energy (mN/m)					
Polar	8.96 ± 0.83	18.88 ± 0.85	3.81 ± 1.03	16.52 ± 0.71	10.87 ± 0.79
Dispersive	32.97 ± 0.56	35.23 ± 0.68	29.63 ± 0.57	36.40 ± 0.54	35.58 ± 0.55
Total	41.93 ± 1.00	54.11 ± 1.09	33.44 ± 1.18	52.91 ± 0.98	46.46 ± 0.96
Cell seeding efficiency (%) (incl statistical significance: (ns) when *p*-value >0.05; (*) < 0.05)					
	128.8 ± 16.9 (ns)	93.1 ± 9.0 (ns)	7.5 ± 5.0 (*)	85.7 ± 13.9 (ns)	77.1 ± 22.3 (ns)

favourable ($\Delta H°_f = -6706$ kJ/mol), and the formation of a very soluble salt, $ZrOCl_2.8H_2O$ ($\Delta H°_f = -3475$ kJ/mol) [9], in the acidic environment provided by the higher concentration of H^+ClO^- [10] led to the sharp decline of Zr content in the oxide layer (Eq. 5). This is in contrast with the samples treated with NaClO only, whose Zr content did not plummet in the oxide layer because $ZrOCl_2.8H_2O$ salt only forms in acidic conditions (i.e., HClO is a weak acid that does not break down in water readily ($\Delta H°_{solution} = +37.49$ kJ/mol). (Thermodynamic data source: [11]).

$$2\ CuCl_2^-{}_{aq} + 2\ OH^- \leftrightarrow Cu_2O + H_2O + 4\ Cl^- \quad (3)$$

$$Zr^{2+} + OH^- \rightarrow Zr(OH)_4 \quad (4)$$

$$Zr^{2+} + ClO^- \text{ (excess)} \rightarrow ZrOCl_2.8\ H_2O \text{ (very soluble)} \quad (5)$$

When the samples were treated with Virkon® solution their oxide layer did not change significantly compared to the untreated samples. A slight decrease of the Cu2p peak (Cu_xO content) and an increase in Zr3d peaks (ZrO_2 content) indicate the oxidising effect of the solution on the surface. This also explains the shoulder in the Cu2p spectrum, attributed to the oxidation of cuprous oxide (Cu_2O) to cupric oxide (CuO) (x = 1→2) (Fig. 1iii).

The surfaces display macroscale and microscopic differences (Fig. 2). The blue hue on the samples treated with NaOH and NaOH/NaClO mixture (Fig. 2ii, iv) confirms the presence of precipitated copper salts (Eq. 1). A micro-scale texturing pattern was present in the NaOH-treated samples (Fig. 2vii, xi). The Cu-enriched micropits in the NaClO (Fig. 2viii, xii) and the mixture-treated samples (Fig. 2ix, xiii) confirm the mechanism for the dissolution of the Cu metal, i.e., Cu-rich zones resulting from the solution of $CuCl/Cl_2$ complexes (Eq. 2). The mixture-treated surfaces presented both pitting and a textured pattern (Fig. 2ix). The samples treated with Virkon® did not show pitting corrosion cavities (Fig. 2x), confirming the safety of the solution for this alloy composition.

The Surface Free Energy (SFE) value (and the contact angle) differed with the disinfectant employed (Table 1). The total SFE was lowest in the NaClO-treated samples, the most hydrophobic surface (contact angle >80°) of the set. These two variables are negatively correlated (Supplementary material). The largest SFE magnitude was measured on the NaOH-treated samples, and they possessed the lowest contact angle and

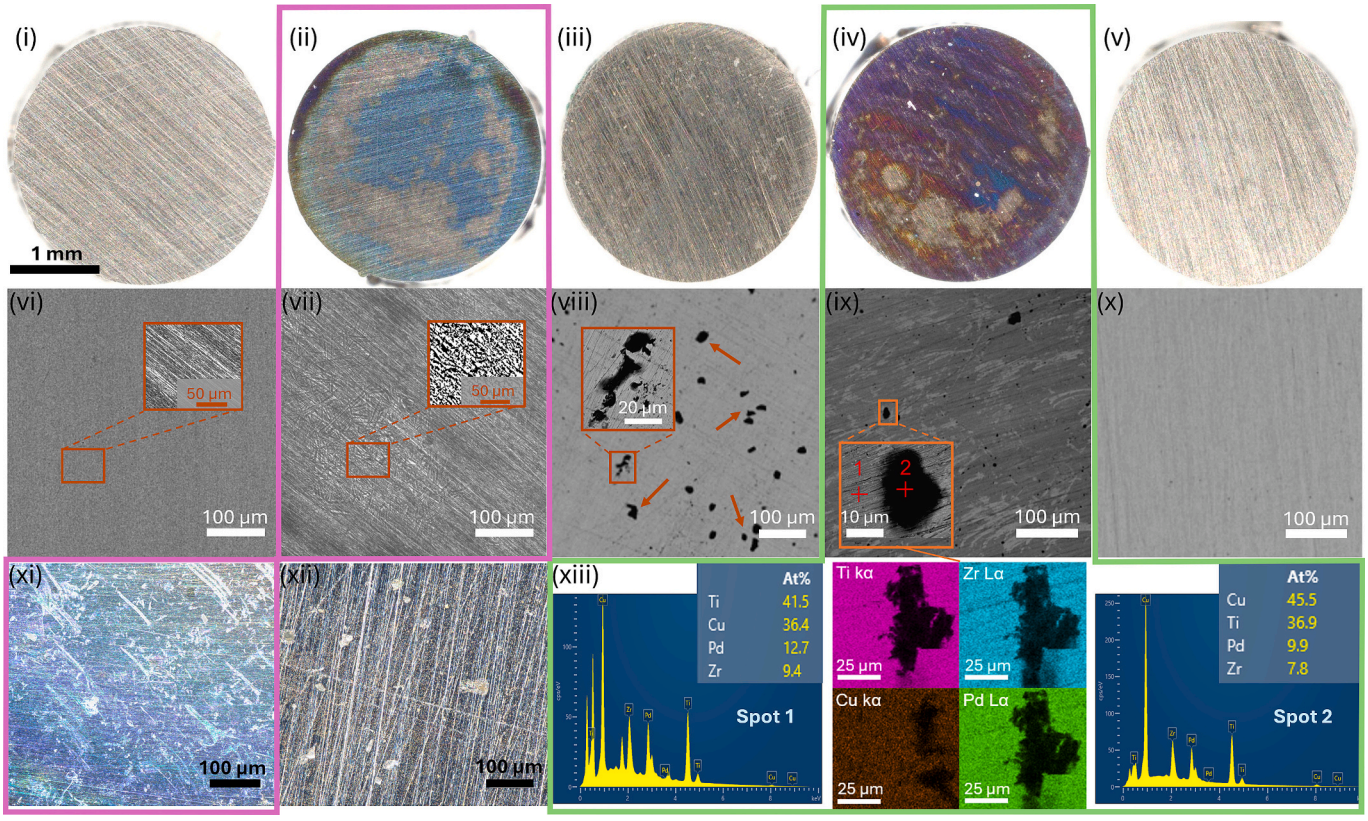

Fig. 2. Optical images and SEM/EDX of the (i, vi) untreated surfaces and treated with (ii, vii, xi) 1 M NaOH; (iii, viii, xii) 1% NaClO; (iv, ix, xiii) 1 M NaOH/1% NaClO mixture; and (v, x) 1% Virkon® solutions.

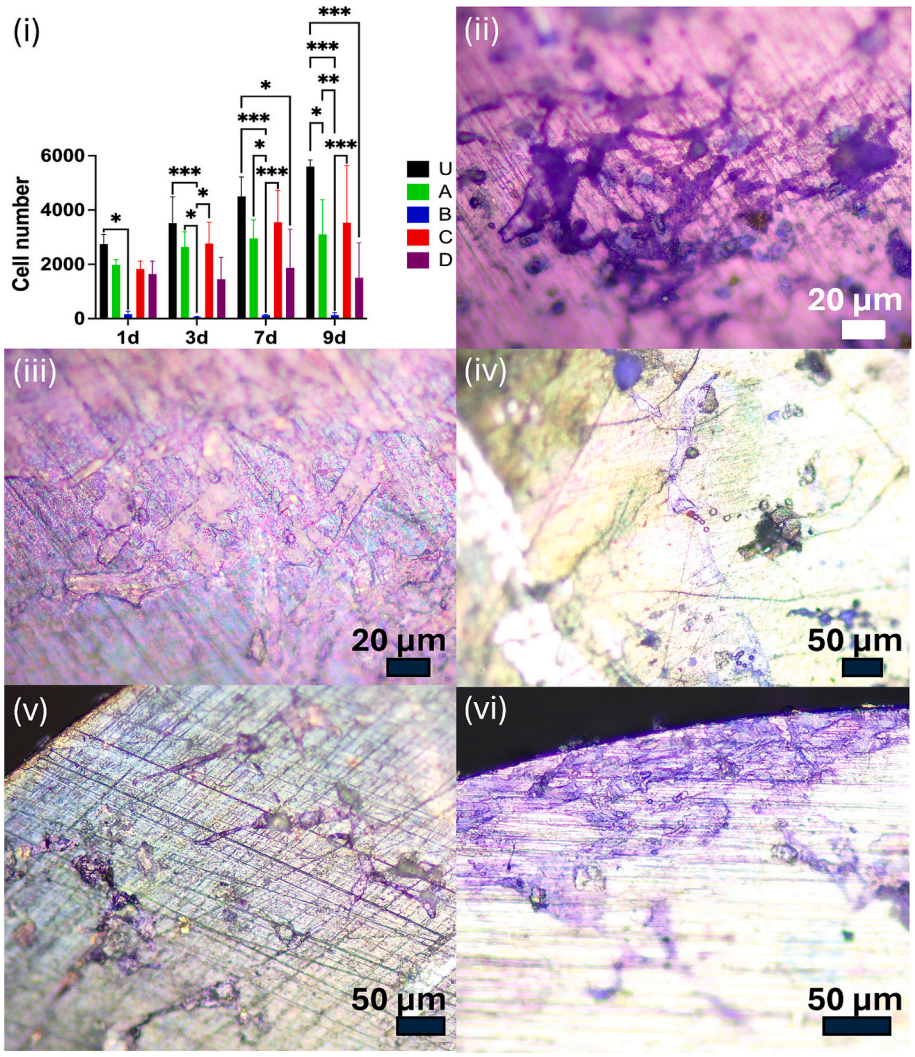

Fig. 3. (i) Cell number on surfaces during proliferation stage; (ii-vi) Pre-osteoblast morphology on day 5 on the untreated surfaces and those treated with NaOH, NaClO, NaOH/NaClO mixture and Virkon®, respectively.

largest at.% of TiO_2 and ZrO_2. The TiO_2 correlation has also been reported [6].

Cell incubation studies offer a functional validation of the effect of these disinfectants. Seeding efficiency was lowest on NaClO-treated surfaces (Table 1). This is attributed to the lowest TiO_2 content and SFE, and highest hydrophobicity (contact angle). The SFE polar component was markedly low and this has been reported to correlate positively with cell seeding efficiency [6]. Cell numbers during the proliferation stage (days 1–9) (Fig. 3i) showed that NaClO-treated surfaces were least conducive to sustain cell growth, with statistical significance. Leached Cu^{x+} ions from the Cu-rich micropits (Fig. 2 viii) contribute to this phenomenon, since Cu is cytotoxic, arrests early mitosis and induces cell death [12]. There exists a positive correlation between cell proliferation, TiO_2 content, SFE and cell seeding efficiency; and negative with Cu_xO, Pd content and contact angle (Supplementary material). The morphology of the osteoblasts captured on day 5 (Fig. 3ii-vi), with stretching pseudopodia, indicate good attachment onto the treated surfaces, though cracked and damaged (Fig. 3iv, v), and the colony sizes match cell number (Fig. 3i).

4. Conclusions

We recommend the use of non-chlorinated disinfection solutions for medical devices made of Ti-Zr-Cu-Pd BMGs. Otherwise, the oxide layer is modified by decreasing TiO_2 or ZrO_2 (components of a robust protective layer), forming Cu_xO-rich pits, reducing SFE and increasing hydrophobicity. Those changes correlate with poor cell behaviour. This study intends to have value to surgery practitioners handling implantable medical devices which require disinfection prior to surgical deployment.

CRediT authorship contribution statement

C. Torres-Sanchez: Writing – review & editing, Writing – original draft, Visualization, Supervision, Resources, Methodology, Investigation, Funding acquisition, Formal analysis, Data curation, Conceptualization. **S. Yang:** Writing – original draft, Visualization, Methodology, Formal analysis, Data curation. **J. Tarum:** Writing – original draft, Visualization, Investigation, Data curation. **P.P. Conway:** Writing – review & editing, Supervision, Resources, Project administration, Funding acquisition.

Declaration of competing interest

The authors declare that they have no known competing financial interests or personal relationships that could have appeared to influence the work reported in this paper.

Acknowledgements

Alloyed Ltd., Wolfson School Bursaries and EPSRC (EP/V007335/1).

Appendix A. Supplementary data

Supplementary data to this article can be found online at https://doi.org/10.1016/j.matlet.2026.140428.

Data availability

Data will be made available on request.

References

[1] P. Meagher, E.D. O'Cearbhaill, J.H. Byrne, D.J. Browne, Bulk metallic glasses for implantable medical devices and surgical tools, Adv. Mater. 28 (27) (2016) 5755–5762, https://doi.org/10.1002/adma.201505347.

[2] H.F. Li, Y.F. Zheng, Recent advances in bulk metallic glasses for biomedical applications, Acta Biomater 36 (2016) 1–20, https://doi.org/10.1016/j.actbio.2016.03.047.

[3] S. Yang, J. Tarum, P.P. Conway, C. Torres-Sanchez, Thermal, Mechanical and Biocompatible Behaviour of a Ti-Zr-Cu-Pd Bulk Metallic Glass with Lower Zr and Pd Content, SSRN (2026), https://doi.org/10.2139/ssrn.5589799.

[4] G. Fichet, E. Comoy, C. Duval, K. Antloga, C. Dehen, A. Charbonnier, G. McDonnell, P. Brown, C. Ida Lasmézas, J.-P. Deslys, Novel methods for disinfection of prion-contaminated medical devices, Lancet 364 (9433) (2004) 521–526, https://doi.org/10.1016/S0140-6736(04)16810-4.

[5] R.M. Clarkson, A.J. Moule, Sodium hypochlorite and its use as an endodontic irrigant, Aust. Dent. J. 43 (4) (1998) 250–256, https://doi.org/10.1111/j.1834-7819.1998.tb00173.x.

[6] C. Torres-Sanchez, E. Alabort, O. Herring, H. Bell, C.Y. Tam, S. Yang, P.P. Conway, Multidimensional analysis for the correlation of physico-chemical attributes to osteoblastogenesis in TiNbZrSnTa alloys, Biomater. Adv. 153 (2023) 213572, https://doi.org/10.1016/j.bioadv.2023.213572.

[7] D.K. Kozlica, J. Ekar, J. Kovač, I. Milošev, Roles of chloride ions in the formation of corrosion protective films on copper, J. Electrochem. Soc. 168 (3) (2021) 031504, https://doi.org/10.1149/1945-7111/abe34a.

[8] G. Kear, B.D. Barker, F.C. Walsh, Electrochemical corrosion of unalloyed copper in chloride media—a critical review, Corros. Sci. 46 (1) (2004) 109–135, https://doi.org/10.1016/S0010-938X(02)00257-3.

[9] N.V. Karyakin, N.G. Chernorukov, A.K. Koryttseva, G.N. Chernorukov, The standard enthalpy of formation of zirconyl chloride octahydrate, Zhurnal Neorganicheskoj Khimii 40 (12) (1995) 2007–2008. https://www.osti.gov/etdeweb/biblio/239799.

[10] K. Matsui, M. Ohgai, Formation mechanism of hydrous-zirconia particles produced by hydrolysis of $ZrOCl_2$ solutions, II, J. Am. Ceram. Soc. 83 (6) (2000) 1386–1392, https://doi.org/10.1111/j.1151-2916.2000.tb01398.x.

[11] NIST, Thermodynamic data source, chemistry WebBook, National Institute of Standards and Technology,Thermodynamic data source, 2025. https://webbook.nist.gov/chemistry.

[12] M.C. Cortizo, M.F.L. de Mele, A.M. Cortizo, Metallic dental material biocompatibility in osteoblastlike cells, Biol. Trace Elem. Res. 100 (2) (2004) 151–168, https://doi.org/10.1385/BTER:100:2:151.